

Observation of the rock slope thermal regime, coupled with crackmeter stability monitoring: first results from three different sites in Czechia (Central Europe)

Ondřej Racek^{1,2}, Jan Blahůt², Filip Hartvich²

5 ¹ Charles University in Prague, Faculty of Sciences, Department of Physical Geography and Geoecology, Albertov 6, 128 43, Prague, Czechia

² Department of Engineering Geology, Institute of Rock Structure and Mechanics, Czech Academy of Sciences, V Holesovickach 94/41, 182 09, Prague, Czechia

Correspondence to: Ondřej Racek (racek@irms.cas.cz)

10 This paper describes a newly designed, experimental and affordable rock slope monitoring system. By this system, three rock slopes in Czechia are being monitored for a period of up to two years. The instrumented rock slopes have different lithology (sandstone, limestone, and granite), different aspect and structural and mechanical properties. Induction crackmeters monitor the dynamic of joints, which separate unstable rock blocks from the rock face. This setup works with a repeatability of measurements 0.05 mm. External destabilizing factors (air temperature, precipitation, incoming and outgoing radiation, etc.)

15 are measured by a weather station placed directly within the rock slope. Thermal behaviour in the rock slope surface zone is monitored using a compound temperature probe, placed inside a 3 m deep sub-horizontal borehole which is insulated from external air temperature. Additionally, one thermocouple is placed directly on the rock slope surface. From so far measured time series (longest one since autumn 2018) we can distinguish differences between the monitored sites annual and diurnal temperature cycles. From the first data, a greater annual joint dynamic is measured in the case of larger blocks, however,

20 smaller blocks are more responsive to short-term diurnal temperature cycles. Differences in the thermal regime between sites are also recognisable and are caused mainly by different slope aspect, rock mass thermal conductivity and colour. These differences will be explained by statistical analyses of longer time series in the future.

Keywords: monitoring, rock slope, stability, temperature, crackmeter, horizontal borehole temperature

1 Introduction

25 The rock slope stability is crucially influenced by both rock properties and exogenous factors (D'Amato et al. 2016, Selby 1980). The rock physical properties are well known and numerous laboratory experiments and theoretical works exist in this field. However, there are very few in-situ experiments that would deal with real-world scales (Fantini et al. 2016; Bakun-Mazor et al. 2013, 2020; Janeras et al. 2017; Marmoni et al. 2020; Isaka et al., 2018). Moreover, all these studies are focused on monitoring of a single, well-known unstable rock slope.

30 Thermal expansion and frost action together with severe rainfall events are the main exogenous physical processes of the mechanical weathering of the rock surface (Krautblatter and Moser, 2009). Together with chemical weathering, these ultimately result in the weakening of the rocks slopes and reduction of their stability (Gunzburger et al. 2005, Vespremeanu-Stroe and Vasile, 2010; do Amaral Vargas et al. 2013; Draebing 2020). The loss of stability, caused by repeated changes in the stress field inside the rock eventually leads to a rockfall, one of the fastest and most dangerous forms of slope processes
35 (Weber et al. 2017, 2018; Gunzburger et al. 2005). In the alpine environment, rock falls are increasingly caused by permafrost degradation and frost cracking (Gruber et al. 2004; Ravelin et al. 2017) or temperature-related glacial retreat (Hoelzle et al. 2017). To address the influence of permafrost melting on the rock slope stability, several monitoring systems/campaigns were proposed. Magnin et al. (2015a) constructed a monitoring system consisting of rock temperature monitoring both on the rock face and in-depth sensors. In-depth rock mass temperature monitoring was placed in up to 10 m deep boreholes. The monitoring
40 was coupled with ERT campaigns to determine sensitive permafrost areas (Magnin et al. 2015b). Girard et al. (2012), introduced a custom acoustic emission monitoring system for quantifying freeze-induced damage in rock. An extensive monitoring system for permafrost activity in Switzerland is presented by Vonder Mühl et al., (2008) and Noetzli and Pellet, (2020). Additionally, a significant percentage of small rock falls is directly triggered by rainfall (Krautblatter and Moser, 2009; Ansari et al, 2015). The linkage between rock fall occurrence and rainfall intensity is, however, not linear and the majority of
45 events are triggered when rainfall intensity exceeds a specific threshold.

Among the destabilizing processes caused by changes in rock temperature and contributing to the decrease of stability are:

- rock wedging-ratcheting (Bakun Mazor et al., 2020; Pasten et al., 2015)
- repeated freeze-thaw cycles
- 50 - thermal expansion-induced strain (Gunzburger et al., 2005; Matsuoka 2008)
- and in specific conditions, exfoliation sheets can be destabilized by cyclic thermal stress (Collins and Stock, 2016; Collins et al., 2017).

These processes are often repeated many times, thus effectively widening the joints and fracturing the rock.

Rock slope monitoring is one of the common tasks in engineering geology, often used at construction sites (Ma et al. 2020, Li
55 et al. 2018; Scaoni et al. 2018), along roads or railways or to protect settlements. Various approaches are used, with a background in geodesy (Gunzburger et al. 2005; Reiterer et al. 2010; Yavasoglu et al. 2020), geotechnics (Greif et al. 2017; Lazar et al. 2018), geophysics (Burjanek et al. 2010; 2018; Weber et al. 2017, 2018; Coccia et al. 2016; Yan et al. 2010; Weigand et al. 2020; Warren et al. 2013), or remote sensing methods (Sarro et al. 2018; Matano et al. 2015). Most commonly, sensors such as thermometers, accelerometers, inclinometers, visible light or IR cameras, total stations, TLS, GbSAR and
60 seismographs are used to detect potential rock fall events (Burjanek et al. 2010, 2018; Tripolitsiotis et al. 2015; Matsuoka, 2019). These methods are more suitable for monitoring large rock slopes. Tiltmeters, extensometers and other geotechnical devices are usually used to monitor a single unstable block/part of the rock slope (Barton et al. 2000; Lazar et al. 2018). Usually, monitoring methods using various sensors are combined. Large rockslides are monitored by Crosta et al., (2017),

Zangerl et al., (2010) and Loew et al., (2012) using the combination of remote sensing, geodetical network and borehole inclinometer. Experimental monitoring systems aim to develop or test new sensors or approaches (Loew et al., 2017; Jaboyedoff et al., 2004, 2011; Chen et al., 2017; Hellmy et al., 2019) or to describe long term processes of rock slope destabilization (Fantini et al., 2016; Kromer et al., 2019; Du et al., 2017). However, these systems are site-specific and installation of a similar system within multiple sites is complicated and often financially demanding.

To quantify the influence of meteorological variables, weather stations should be included within monitoring systems (Macciotta et al., 2015). Rarely, environmental monitoring is supplemented by solar radiation monitoring (Gunzburger and Merrien-Soukatchoff, 2011). Thermal observations are often limited to air temperature and/or rock face temperature monitoring only (Jaboyedoff et al. 2011, Blikra and Christiansen, 2014; Marmoni et al. 2020; Collins and Stock, 2016; Collins et al. 2017; Eppes et al. 2016). Less commonly, the temperature changes are measured within the rock mass depth (Magnin, et al. 2015a, Fiorucci et al. 2018). Site-specific designed systems are difficult to modify and usually expensive. This brings difficulties into data processing because they are locally biased and cannot be directly compared.

Therefore, an easy-to-modify, modular and affordable monitoring system composed of crackmeters, weather station, solar radiation and compound borehole temperature probe has been designed and tested. With just minor modifications, various rock slope sites can be easily instrumented, allowing to compare data about rock slope temporal behaviour in different settings, potentially bringing new, much needed data about rock slope stability spatiotemporal development (Viles, 2013).

80 **2 Monitoring methods**

The rock slope monitoring methods have recently gone through a massive development concerning precision, accuracy, reliability, sampling rate, and applicability (Tables 1, 2). Even completely new methods were established, for example, unmanned aerial vehicles applications, high precision or UAV held TLS, etc. This expansion was mostly allowed by the rapid development of corresponding fields of informatics, computation technologies, communication channels and satellite technology applications.

Unlike the above-mentioned systems, the monitoring system presented here (Fig. 1,2; Table 1), can be placed at various sites without major modifications. Using common safety rules and methods for working in heights, the system can be placed directly within vertical or even overhanging rock face. Anchoring must be placed within a stable part of the rock slope, which ensures worker's safety under any circumstances. This monitoring design brings an opportunity to compare results from different locations and observe generally applicable regularities in rock face thermo-mechanical behaviour thanks to the same instrumentation on various rock slope sites. All sensors were calibrated by the manufacturer before they were installed on the rock slope to provide precise data. The monitoring system (Table 1, Fig. 1) is composed of the following components:

- a set of automatic induction crackmeters, coupled with dataloggers (Fig. 1) measuring relative block displacement

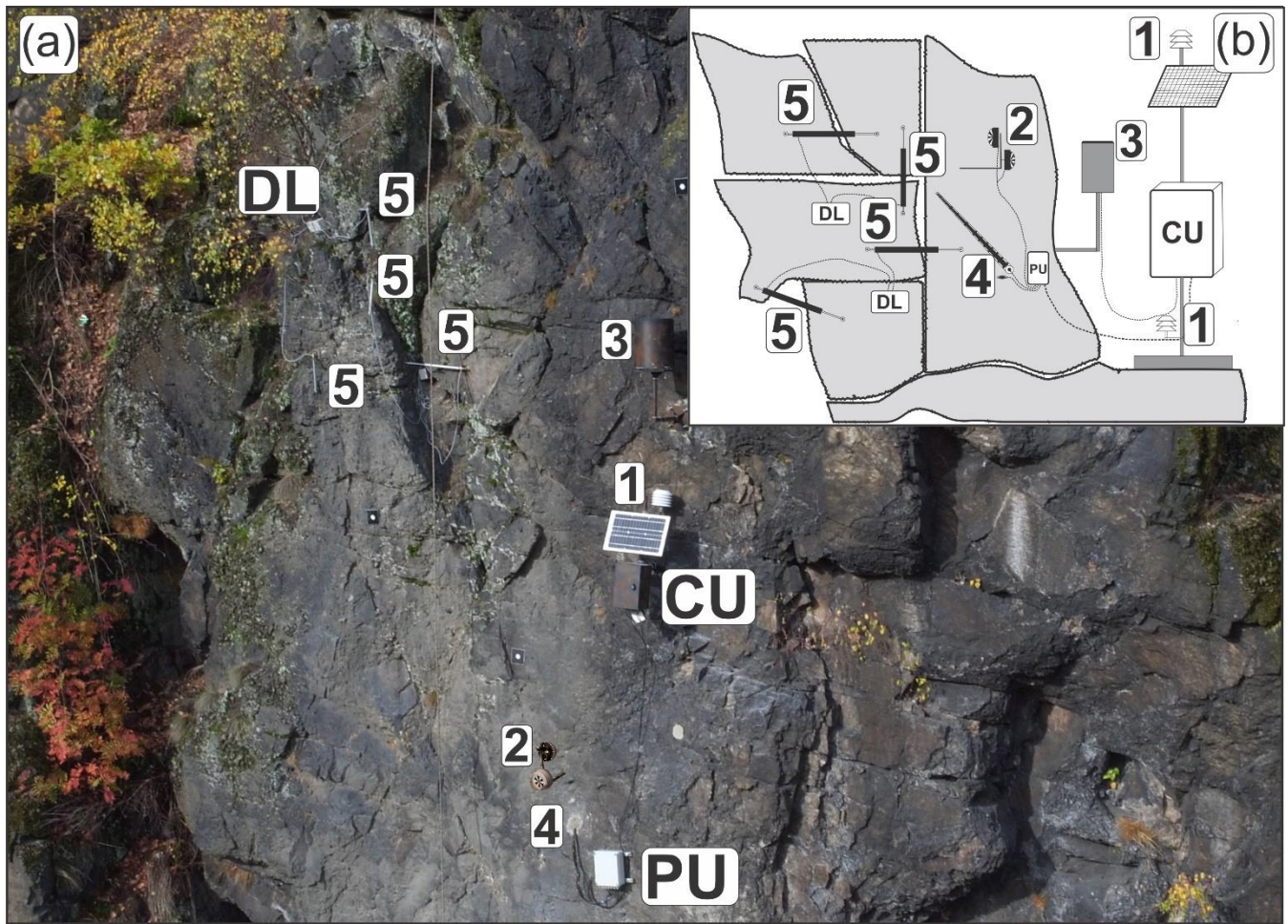
- a weather station with a set of sensors measuring various meteorological data (Fig. 1), such as air temperature, humidity and pressure (Table 1), and rock slope surface solar radiation balance (incoming/reflected radiation) of the rock face (Fig. 5) using a pair of pyranometers
- a set of 12 thermocouples placed along a 3 m deep borehole (Fig 2.), carefully insulated between each neighbouring sensor, measuring rock slope temperature in-depth profiles

| Component | Manufacturer | Accuracy | Resolution | Repeatability | Measuring range | Max sampling rate | Protection | Operational temperature | Service life | Price |
|------------------------------------|--------------------|----------|-----------------------|---------------|--------------------------------------------|-------------------|-----------------|-------------------------|-----------------------------|---------|
| Crackmeter Gefran PZ 67-200 | GEFRAN (It) | <0.1 % | 0.05 mm | 0.01 mm | 0-200 mm | N/A | IP67 | -30 - 100 °C | > 25*10 ⁸ m str. | 300 € |
| Datalogger Tertium Beacon | Tertium tech. (It) | N/A | N/A | N/A | N/A | < 1 sec | IP65 | -30 - 60 °C | > 5 years | 190 € |
| Datalogger Temp. Sensor | Tertium tech. (It) | 0.02 °C | 0.01 °C | N/A | -30 - 60 °C | < 1 sec | IP67 | -30 - 60 °C | > 5 years | |
| Control unit, battery, solar panel | FIEDLER (Cz) | N/A | 0.00X; 16bit | N/A | N/A | 1 min | IP66 | -30 - 60 °C | > 5 years | |
| Temperature sensor | FIEDLER (Cz) | 0.1 °C | 0.1 °C | 0.01 °C | -50 - 100 °C | 1 min | IP66 | -50 - 100 °C | > 5 years | |
| Rain gauge SR03 500cm2 | FIEDLER (Cz) | 0.05 mm | 0.1 mm/year | 0.1 mm | N/A | 50 m. sec | IP66 | 0 - 60 °C | > 5 years | 1 650 € |
| Humidity sensor | FIEDLER (Cz) | 0.008 % | < 0.1 %/year | 0.02 % | 0 - 100 % | 1 min | IP66 | -50 - 100 °C | > 5 years | |
| Atmospheric pressure sensor | FIEDLER (Cz) | 2 mbar | 0.025 mbar | 0.1 mbar | 300 - 1100 mbar | 1 min | IP66 | -40 - 70 °C | > 5 years | |
| Pyranometer SG002 | Tlusták (Cz) | 10%/day | 20 µV/Wm ² | < 5% | 300 - 2800 nm (0 - 1200 W/m ²) | 1 min | IP66 | -30 - 60 °C | > 5 years | 450 € |
| Borehole temperature sensor | FIEDLER (Cz) | 0.1 °C | 0.1 °C | 0.01 °C | -50 - 100 °C | 1 min | sealed/cemented | -30 - 60 °C | > 5 years | 1 150 € |
| Datastorage/processing | FIEDLER/SigFox | / | / | / | / | 1 hour | / | / | infinite | 200 € |

100 **Table 1: List of presented monitoring system components, with performance metrics and prices.**

All the elements of the system (Table 1) are commercially available at affordable expenses (one site instrumentation costs approx. 5000 Eur) and are easy to replace by moderately experienced users. Additional costs are the drilling works (1000-2 000 EUR). The cost of borehole drilling depends on the site accessibility and rock mass hardness. The price of the specific monitoring system is also affected by the number of used crackmeters and data loggers. System maintenance costs are not higher than 300 EUR per year including data transmission, processing and storage. This makes the system ideal to be used on multiple sites, without great financial demands. When using the same instrumentation, data from different rock slope sites can be compared and analysed to better understand general rock slope spatiotemporal behaviour.

105



110 **Figure 1: Photo of monitoring system at Tašovice site (a). Generalized scheme of the monitoring system (b). CU: control unit, PU: processing unit, DL: data logger, 1.: Temperature sensor, 2.: Pyranometers, 3.: Rain gauge, 4.: Borehole compound temperature probe, 5.: Crack meters (only four of total six crackmeters are visible on this photo)**

2.1 Dilatation monitoring

At each site, suitable joints separating unstable rock blocks were selected. Joints and subsequent crackmeter placements were selected to best represent general directions of expected rock blocks destabilization. Where it was possible, joints that directly separate unstable blocks from stable rock were chosen. These joints were afterwards instrumented with calibrated induction crackmeters Gefran PZ-67-200. Crackmeters can record movements smaller than 0.1 mm (Tables 1,2). In comparison with other methods measuring spatial change, their precision is high, with lower costs (Table 2). The temporal resolution of the measurement is nearly continuous when the crackmeter position can be read every second (Table 2). Moreover, we have tested these in a controlled temperature environment using a climate chamber to find out any temperature-dependent errors. In this controlled test, we were able to measure the expansion of a concrete block. The resulting block expansion measurements matched the theoretically calculated concrete block expansion. This way we made sure, that

115
120

measurement of the crackmeters is not biased by dilatation of the device itself. Crackmeters are suitable for harsh conditions (Table 1). The devices can withstand temperature changes, snow cover, ice accumulation or rainfall with IP 67 protection. Crackmeters are coupled with Tertium Beacon dataloggers (Tertium technology, 2019), which contain accurate in-situ temperature sensors (Table 1). When a datalogger is placed within the discontinuity, it records local temperature. The joint dilatation and temperature data are stored in the datalogger and can be wirelessly transmitted at a distance of up to a hundred meters using wi-fi, which simplifies data collection as it can be usually performed from below the rock face. Tertium Beacon data can be sent to a server via IoT SigFox network. The crackmeters and dataloggers are powered with two AA batteries, which last typically 6-12 months according to local climate. The displacement and temperature are set to be measured every hour. This can however be changed, if necessary, e.g., during special experiments such as thermal camera monitoring campaigns (Racek et al. 2021).

| Method | Results | Range | Precision | Sampling rate | Online data | Price |
|-----------------------------|--------------------|-----------|-------------|----------------|-------------|-----------|
| Induction crack meter | 1D distance | < 1 m | 0.01 mm | seconds-days | yes | 300 € |
| Precision tape | 1D distance | < 30 m | 0.5 mm/30 m | hours-days | no | 800 € |
| Fixed wire extensometer | 1D distance | 10 - 80 m | 0.3 mm/30 m | hours-days | yes | 4 000 € |
| Rod for crack opening | 1D distance | < 5 m | 0.5 mm | hours-days | no | 300 € |
| LVDT | 1D distance | < 0.5 m | 0.25 mm | seconds-days | yes | 170 € |
| Laser dist. meters | 1D distance | < 1000 m | 0.3 mm | seconds-days | yes | 1 500 € |
| Portable rod dilatometer | 1D distance | < 1 m | 0.1 mm | hours-days | no | 350 € |
| Total station triangulation | 3D distance | < 1000 m | 5 - 10 mm | hours-days | yes | 3 000 € |
| Precise levelling | 1D distance | < 50 m | < 1 mm | days | no | 350 € |
| EDM | 1D distance | 1 - 15 km | 1 - 5 mm | minutes - days | no | 10 000 € |
| Terrestrial photog. | 3D distance | < 100 m | < 20 mm | minutes-days | yes | 1 000 € |
| Aerial photog. | 3D distance | < 100 m | 10 - 100 mm | hours-days | no | 1 500 € |
| Tiltmeter | inclination change | ±10° | 0.01° | seconds-days | yes | 300 € |
| GPS | 3D distance | Variable | < 5 mm | seconds-days | yes | 2 000 € |
| TLS | 3D distance | Variable | 5 - 100 mm | minutes-days | yes | 100 000 € |
| GB InSAR | 3D distance | Variable | < 0.5 mm | minutes-days | yes | 100 000 € |

Table 2: A comparison of rock slope spatial change monitoring techniques (updated after Klimeš et al., 2012)

2.2 Environmental monitoring

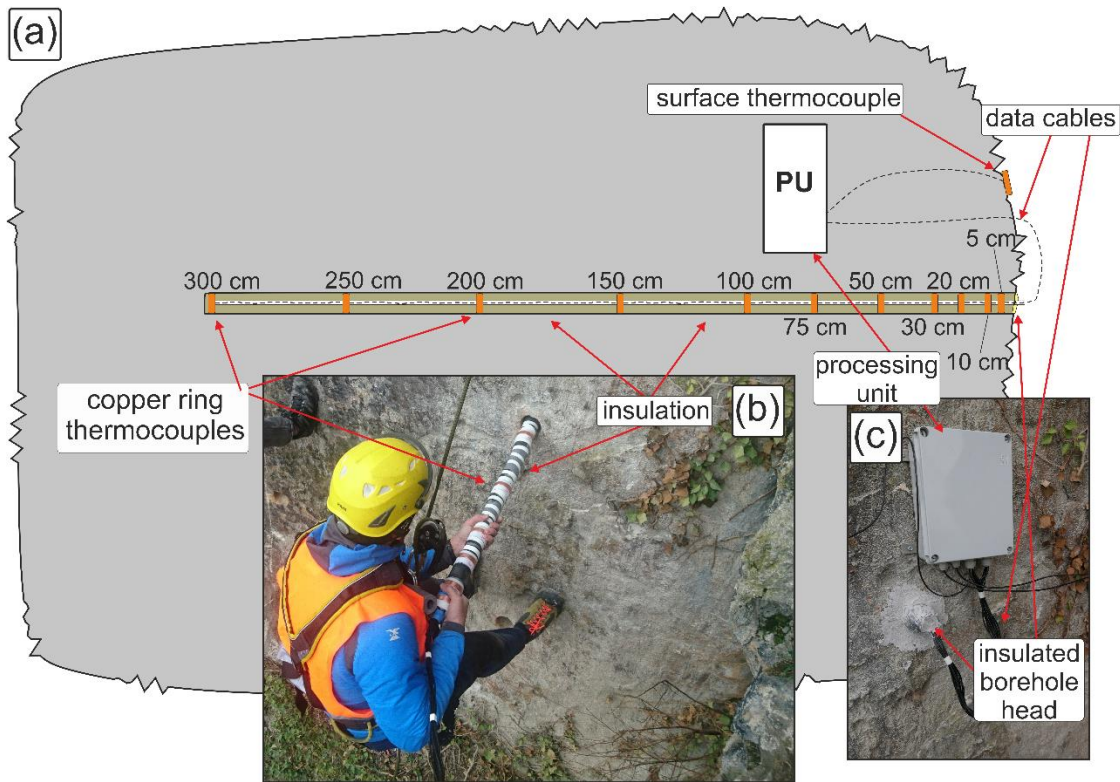
For the monitoring of the weather and climatic parameters at the sites of interest, we use automatic weather stations manufactured by Fiedler environmental systems. These are composed of a registration, communication and control unit, an external tipping-bucket rain gauge, two temperature sensors, an atmospheric pressure sensor, a humidity sensor, and a pair of pyranometers, measuring the incoming and reflected solar radiation. All these sensors and the control unit are powered by a 12 V battery, which is charged by a small solar panel (Fig. 1). Except for precipitation, which is measured using a pulse signal, all other meteorological variables and solar radiation are measured every 10 minutes. The control unit is equipped with a GSM

modem, which sends the data automatically to the server of the provider every day. For detailed information about accuracy, durability and price of environmental monitoring see table 1.

To compute the radiation balance (incoming minus reflected solar radiation) of a rock face, it is necessary to measure with two opposite facing pyranometers. For this purpose, a set of pyranometers is used (Gunzburger and Merrien-Soukatchoff, 2011; 145 Janeras et al. 2017; Vasile and Vespremeanu-Stroe, 2017), pyranometers are placed perpendicular to the rock face, one facing the rock surface while the other faces the sky hemisphere. This setup enables the measurement of both incoming and reflected solar radiation. The sensors are not placed directly on the rock face, but on an L-shaped holder, which allows placing both sensors almost at the same point (Fig. 1). The rock-facing pyranometer is placed at a distance of approx. 10 centimetres from the rock surface. The pyranometers have an output of 0–2 V, which corresponds to a global radiation of 0–1200 W/m³. 150 Monitored wave length spans from 300 to 2800 nm. Outputs from pyranometers are processed by a converter and then sent with the other monitored meteorological variables to the data hosting server.

2.3 Borehole temperature monitoring

For the monitoring of the thermal behaviour of a rock slope, it is necessary to know temperatures at different depths of the rock mass. The newly designed in depth compound temperature probe (Fig. 2) is a crucial part of our monitoring system. 155 The sensors are placed in a 3 m deep sub-horizontal borehole. To ensure safety during drilling and the long lifespan of borehole and sensors, the borehole itself is drilled to the stable part of the rock slope. The borehole is then equipped with a custom-designed probe with a set of thermocouples. Technical parameters of temperature sensors are the same as for air temperature sensors (Tab 1). Thermocouple sensors that are connected to copper rings are originally designed for soil temperature measurement. By connecting these to copper rings, they are suitable to measure the temperature of borehole walls. Copper 160 rings with 5 cm diameter are placed at a given distance on the tubular spine (5 cm below the surface, 10 cm, 20 cm, 30 cm, 50 cm, 75 cm, 100 cm, 150 cm, 200 cm, 250 cm and 300 cm). The probe is placed in the sub-horizontal borehole, so copper rings containing temperature sensors lay directly on borehole walls (Fig. 2). This ensures that the probe is measuring directly the rock mass temperature. Additionally, one thermocouple is placed directly on the rock surface (Fig. 2). The head of the borehole is insulated to prevent air and water inflow into the rock and the sensors inside the borehole are separated by thorough thermal 165 insulation to ensure that the temperatures are not affected by the air circulation inside the borehole. Therefore, temperature readings from the borehole compound probe corresponds with in situ rock mass temperature. The thermal data, collected every 10 minutes, are passed through a converter and send to the main control unit of the environmental station.



170 **Figure 2: Compound borehole thermocouple probe. (a): generalised scheme, (b): photo of compound thermocouple probe installation, (c): insulated head of sub-horizontal borehole with a processing unit.**

3 Instrumented sites

The monitoring system has been so far established at three different sites (Fig. 3), using the same instrumentation setup. The sites were chosen deliberately in steep rock slopes built of various rock types, with various slope aspect and diverse geological history. To integrate practical application aspect sites were chosen, where the potential rockfall endangers buildings, infrastructure or other social assets.

175

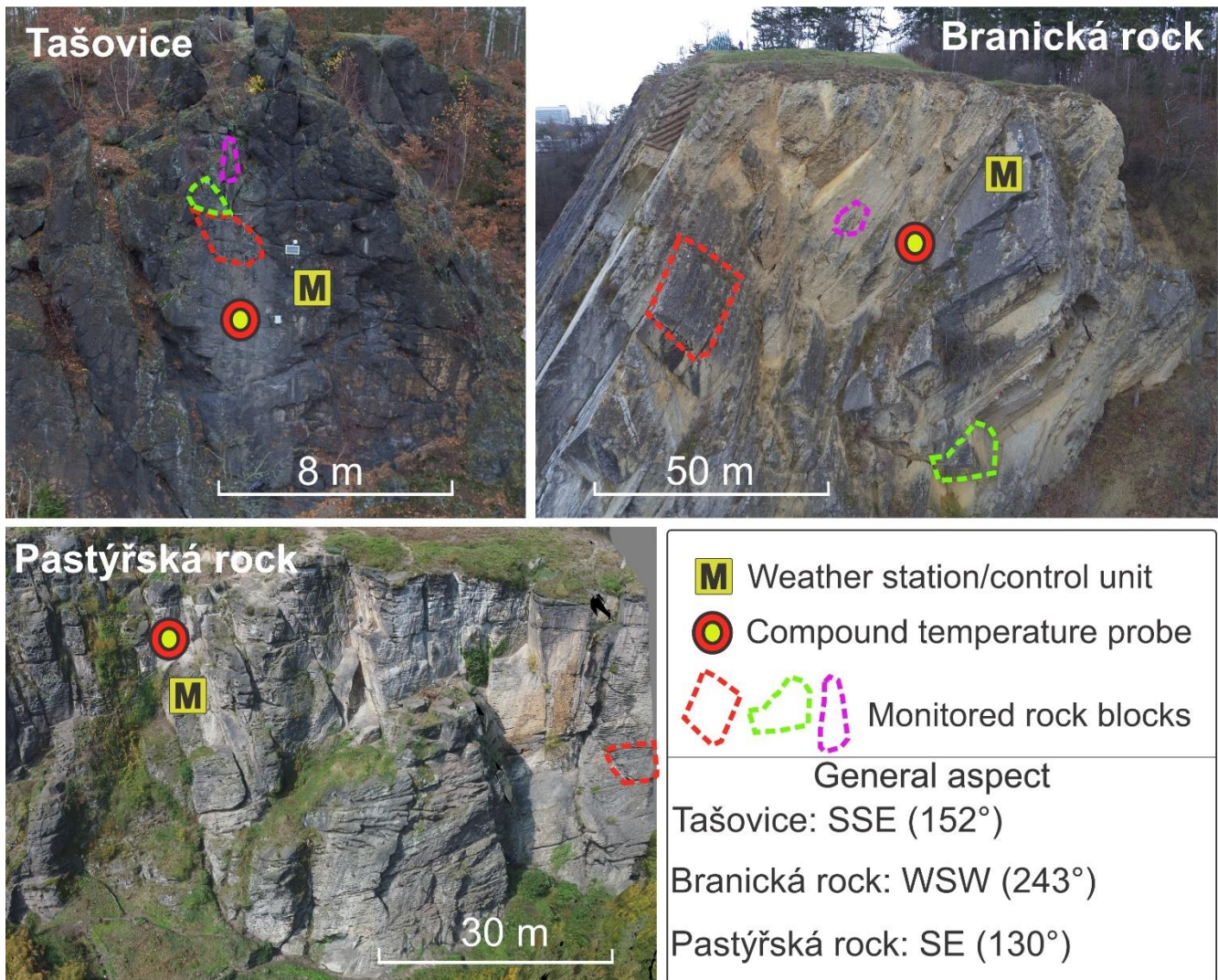


Figure 3: Three instrumented rock slope sites. On each photography the monitored rock blocks are indicated (with dashed lines of different colour), placement of the compound borehole temperature probe and weather station are also indicated.

180 3.1 Pastýřská rock (PS)

The first instrumented rock slope called “Pastýřská rock” is located on the Elbe riverbank in Dečín town, NW Czechia. Monitoring of meteorological variables started in late 2018 (Appendix A). Shortly after that crackmeters and in-depth borehole temperature probe were installed. Pastýřská rock is formed by Cretaceous sandstone with various mechanical properties (Table 3) and has a general SE orientation. The rock slab with the pyranometers and borehole is dipping 87° towards the east (085°).

185 Three main discontinuity sets (80/040, 86/310, 80/275) were identified using geological compass measurements. The locality

is known for extensive rock fall activity in the past, which led to rock slope stabilization works in the late 1980s. However, the block monitored by the crackmeters remained in its natural state. One block is monitored using two pairs of crackmeters. The block has a dimension of 6.7 x 10.7 x 2.5 m and is located in the overhanging part of the rock slope. All four visible cracks are monitored. The colour of the rock slope surface varies from dark, to light grey. The rock slab, where the pyranometers are placed is coloured in light grey colour.

3.2 Branická rock (BS)

This rock slope in Prague (Central Czechia) was instrumented in summer 2019. Rock slope is formed by several Silurian and Devonian limestone layers with varying mechanical and physical properties (Table 3). The rock slope was artificially created by mining (including blasting) and it was used till the 1950s as a limestone quarry. The rock slope is located on a Vltava riverbank and it is generally facing WSW. The pyranometers and the borehole temperature sensors are placed on a rock slab dipping 80° to the SW (235°). Three main discontinuity sets 50/325, 90/197 and 62/085 were identified directly in field. The site is known for extensive rock fall activity in the past, even after quarry closing, which resulted in partial stabilization of known unstable blocks in the 1980s. Three unanchored blocks (Fig. 3) are monitored with seven crackmeters. In the upper part of the rock slope lies the largest monitored block at this site, with dimension 0.9 x 4.5 x 3.7 m. This block is monitored with three crackmeters. The second block is located at the bottom part of the rock slope, partly shaded by vegetation. Dimension of the second block is 2.5 x 1.6 x 3.6 m. This block slowly slides on the bottom surface and is instrumented with two crackmeters. The third monitored block is smaller (0.8 x 1.4 x 0.4 m). It is located in a highly weathered part of the rock slope and monitored with two crackmeters. The colour of limestone varies from grey to yellow and the colour of limestone facing the pyranometer is light grey.

3.3 Tašovice (T)

The third instrumented site is a rock slope above a local road and the Ohře river near Karlovy Vary in W Czechia. The rock slope is formed by partly weathered granite (Table 3). Generally, it is facing SSE direction. The instrumented slab is dipping 88° to the S (170°). Three relatively poorly developed discontinuity systems (50/090, 50/220 and 88/345) were identified. At this site, small rock falls are frequent as it can be seen from the fresh rock and debris accumulation under the rock face. The locality was fully instrumented in spring 2020. Three relatively small blocks are monitored at this site. Block 1 (1.7 x 1 x 2.1 m), Block 2 (0.9 x 0.8 x 0.4 m) and Block 3 (0.5 x 1.2 x 0.4 m). Each block movement is monitored with a pair of crackmeters. The colour of the rock slope varies from black to dark grey. The granite surface at the pyranometers site has a dark grey colour.

4 Fieldwork campaigns

Each instrumented rock slope was characterized using traditional geological, geomorphological and geotechnical methods, such as measuring geometrical properties of joints and fault planes, relative surface strength measurement using a

Schmidt hammer, discontinuity density measuring, and stability estimates using geotechnical classifications (Racek, 2020). Mechanical and physical properties of rock samples (Table 3) will serve as inputs to numerical models of thermally induced strain, which are constructed using Multiphysics ELMER (Raback and Malinen, 2016) and FEATool (FEATool, 2017) software.

| site | samples | ultrasound testing (wet samples) | | | | | pressuremeter (dry samp.) | | | | | Brazilian test (dry samp.) | |
|----------------------------|-------------|----------------------------------|-------------|-------------|-------------|-------------|---------------------------|-------------|-------------|-------------|--------------|----------------------------|------------|
| | | ρ [g/cm ³] | E [GPa] | ν [GPa] | ν | K[GPa] | hardness [MPE [GPa] | μ [GPa] | ν | K [GPa] | Fmax [kN] | σ_t [MPa] | |
| Pastýřská rock (sandstone) | unweathered | 1.87 - 1.92 | 13.8 - 17.4 | 5.8 - 7.7 | 0.12 - 0.26 | 6.6 - 10.4 | 22.3 - 28.5 | 14.8 - 17.2 | 6.2 - 6.9 | 0.17 - 0.24 | 7.6 - 11.2 | 3.0 - 5.5 | 1.3 - 2.4 |
| | weathered | 1.81 - 1.99 | 8.5 - 15.8 | 3.7 - 6.3 | 0.14 - 0.28 | 4.1 - 11.9 | 3.9 - 11.0 | 2.2 - 6.0 | 1.0 - 2.4 | 0.24 - 0.39 | 3.9 - 4.0 | 0.7 - 3.6 | 0.3 - 1.6 |
| Branická rock (limestone) | unweathered | 2.68 - 2.69 | 75.1 - 79.6 | 29.2 - 30.8 | 0.28 - 0.29 | 58 - 61.9 | 77.1 - 244.6 | 65.8 - 75.0 | 24.9 - 29.0 | 0.28 - 0.41 | 50.7 - 129.7 | 14.1 - 36.1 | 5.9 - 15.6 |
| | weathered | 2.67 - 2.69 | 73.4 - 78.1 | 27.9 - 30.2 | 0.29 - 0.34 | 62.2 - 64.3 | 88.2 - 170.5 | 63.6 - 73.1 | 24.4 - 28.2 | 0.27 - 0.31 | 49.3 - 61.0 | 18.1 - 33.4 | 7.8 - 14.0 |
| | with cracks | 2.67 - 2.69 | 64.5 - 78.4 | 24.4 - 30.3 | 0.29 - 0.32 | 60.4 - 63.4 | 52.1 - 192.3 | 25.4 - 74.0 | 9.6 - 27.9 | 0.27 - 0.33 | 24.7 - 61.2 | 11.4 - 26.9 | 4.7 - 10.9 |
| Tašovice (granite) | weathered | 2.39 - 2.52 | 5 - 11.9 | 1.8 - 4.2 | 0.39 - 0.42 | 7.6 - 22.7 | 36.1 - 63.1 | 4.3 - 15.0 | 1.6 - 5.6 | 0.27 - 0.41 | 4.4 - 20.4 | 6.5 - 11.2 | 2.4 - 5.0 |

Table 3: Mechanical and physical properties of laboratory tested rock samples from the three monitored sites. ρ : density, E: Young's modulus, ν : Poisson's ratio, μ : shear modulus, K: bulk modulus, Fmax: maximal axial force, σ_t : max tensile strength. At sites were collected unweathered and weathered samples. At Tašovice site, only weathered granite was available and at Branická rock site some samples contained cracks.

225 Traditional methods were supplemented with state-of-the-art methods of rock slope analysis, including analyses of 3D point clouds and derived mesh surfaces, based on SfM (structure-from-motion, a photogrammetric technique to calculate 3D point cloud from overlapping photos with varying focal axis orientation) (Westoby et al. 2012) processing using the data collected with a UAV or based on TLS. The detailed rock surface models are then analysed using CloudCompare and its plugins (Facets and Compass) (Girardeau-Monaut, 2016; Thiele et al. 2018; Dewez et al. 2016) and the Discontinuity sets 230 extractor (DSE) software (Riquelme et al. 2014) to derive the joint and fault planes and to measure their spatio-structural properties (Fig. 4). These methods automatically (DSE, Facets) or semi-automatically (Compass) derives structural planes from 3D point clouds. From these structural setting and discontinuity systems of rock slope can be determined. Discontinuity sets define partial blocks which form rock slope surfaces.

235

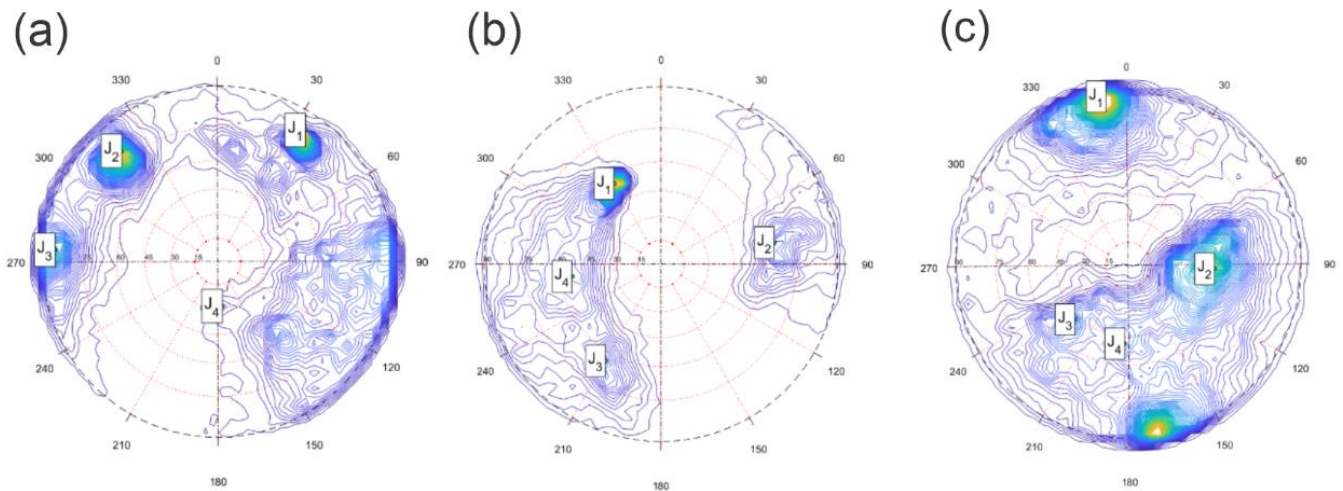


Figure 4: Stereonets with four main discontinuity sets (J1 – J4) classified using DSE software (Riquelme et al. 2014). The density of principal poles corresponds to main discontinuity sets identified from point clouds. (a) Pastýřská rock, (b) Branická rock, (c) Tašovice.

240 5 First results

The monitoring systems are operational for one to two years. During most of the period, the gauges and sensors operated without problems or interruptions. However, some accidents or breakdowns occurred, the most serious being the destruction of one pyranometer by debris, washed down by a rainstorm at Branická rock. As the experimental sites are easy to reach and spare parts easy to obtain, any broken or damaged elements can be replaced within a few days.

245 From the discontinuity analyses it is visible (Fig. 4), that in the case of Pastýřská and Branická rocks the discontinuity systems are clearly defined. Discontinuity sets are in the case of these sites defined mainly by sedimentary layers and cracks perpendicular to them. In the case of Tašovice, discontinuity systems are less pronounced. On this rock discontinuities are linked mainly with tectonically-predisposed weak zones and weathered parts of granite rock. Mechanical properties of rock mass samples (Table 3) differ significantly according to the degree of weathering. Best results in case of the hardness were measured for unweathered limestone at the Branická rock site. The lowest hardness shows weathered sandstone at the Pastýřská rock site. At Tašovice, due to the high degree of weathering of the whole rock slope, we were not able to collect unweathered samples.

5.1 Environmental monitoring

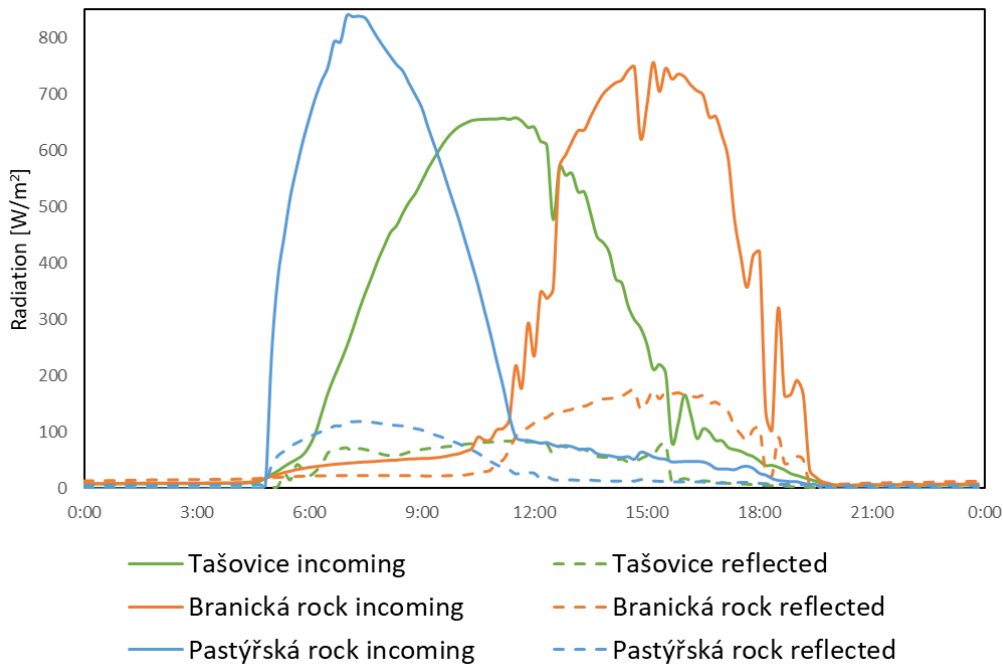
255 Weather station monitoring on all instrumented sites works without problems. From measured time-series of meteorological variables the rock slope microclimate can be defined and the influence on the monitored discontinuity positions can be determined using statistical analyses. The comparison of crack opening with measured rainfall events does not indicate any visible influence of precipitation on the crack opening/closing. However, the measuring period is still short, with prevailing

dry, relatively warm weather. Conversely, there is a visible influence of air and rock mass temperature to block dilatation (Racek et al., 2021), where both diurnal and annual cycles can be identified.

260

5.2 Rock surface radiation balance

Monitoring of rock surface solar radiation balance was installed at monitored rock slopes during 2020 (Branická rock: January, Pastýřská rock February; Tašovice December). Even from these incomplete data we can observe the differences between individual sites (Fig. 5). Local conditions influence incoming radiation pattern by general aspect of the rock slope (temporal shift of incoming radiation peak), rock slope albedo or by shading effects of the pyranometer's surroundings. Differences in the absolute reflected radiation are mainly caused by the different colour of rock faces, and by the different angle of incoming solar radiation due to the aspect of the instrumented slab.



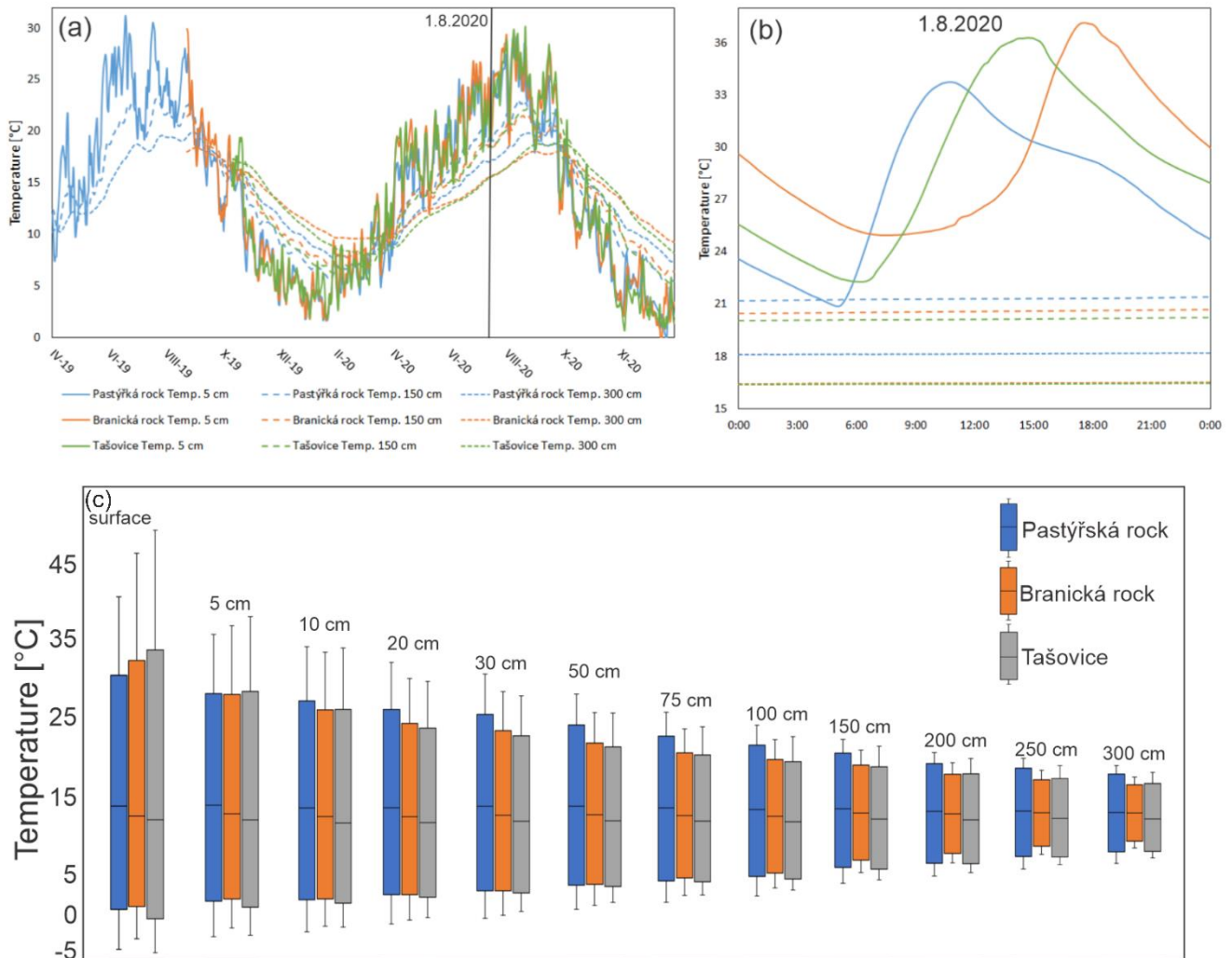
270 **Figure 5: Example of the incoming and reflected radiation measured by pyranometers at Branická rock, Tašovice and Pastýřská rock sites. 24-hour time series of incoming and reflected radiation is displayed. Data were recorded on 1.8.2020 with no clouds. The influence of slope aspect is obvious from the incoming radiation peak shift.**

5.3 Borehole temperature

By continuous temperature measuring in different depths inside a sub-horizontal borehole, we can observe both diurnal and annual temperature amplitude in various depths (Fig. 6). In-depth measurements of temperature show differences

275

in temporal thermal behaviour between monitored rock slopes (Fig.6). From boxplots that represents data from all monitored sites, it is visible that the largest surface temperature variation has been measured at the Tašovice site. This is probably caused by the dark colour of the Tašovice rock surface, with lower albedo. However, in greater depths, this variation decreases. This is probably caused by the lower thermal diffusivity of the granite. Moreover, in the depth of the rock mass the influence of direct sunlight is attenuated. Greater in-depth temperature variation is present at the Pastýřská rock site. However, these data can be biased by different time-series lengths (1 vs 2 full years). The effect of different aspect is visible in the peak of diurnal temperature, when temperature peaks earlier on the E facing rock slope (Pastýřská rock) then on SSE facing Tašovice and WSW facing Branická rock (Fig. 6). Differences in lithology (different thermal diffusivity) cause temporal shift between surface and subsurface temperature peaks. This temporal shift differs between the different rock slopes. A higher median of the in-depth temperature at Pastýřská and Branická rocks (Fig. 6) is caused by longer in-depth temperature time-series spanning over two summer periods.



290 **Figure 6: Comparison of temperatures in different rock slope depths (5, 150 and 300 cm) at three monitored rock slopes. (a) long-term data (daily average), (b) one day data from 1.8. 2020. In depth annual (a) and diurnal (b) temperature amplitude is displayed. (c) in – depth rock mass temperature data from all three monitored sites. Boxplots shows median, minimum, maximum, first and third quartile of temperature data. Temperature amplitudes from compound borehole temperature probe can be compared between sites. At all sites, temperature amplitude decrease with depth is apparent.**

5.4 Blocks dilatation

295 At all monitored sites, the thermally-induced dilatation of individual blocks is observed. However, due to relatively short time-series, the measured crack movements do not yet show any irreversible trends visible on graphs. From the crackmeters data, diurnal and annual amplitudes of crack opening can be identified for all monitored rock blocks. Fig. 7 shows measured diurnal and annual rock crack opening at Pastýřská rock site. From the graph, it is visible the influence of diurnal and annual temperature changes on the crackmeter position. Similar behaviour is observed within all monitored blocks.

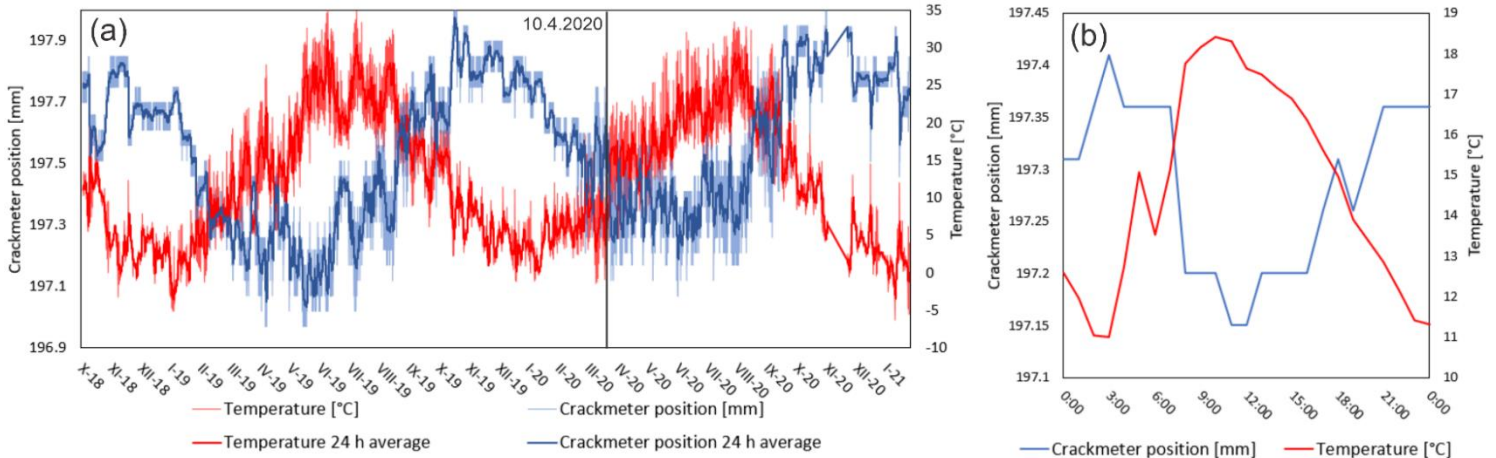


Figure 7: Measured in situ temperature and crack opening at Pastýřská rock site. (a) whole time-series with annual amplitude, (b) example of diurnal amplitude measured on 10.4.2020. From plot (a) annual temperature and crack meter position amplitude can be observed. Plot (b) displaying diurnal temperature and crackmeter position amplitude.

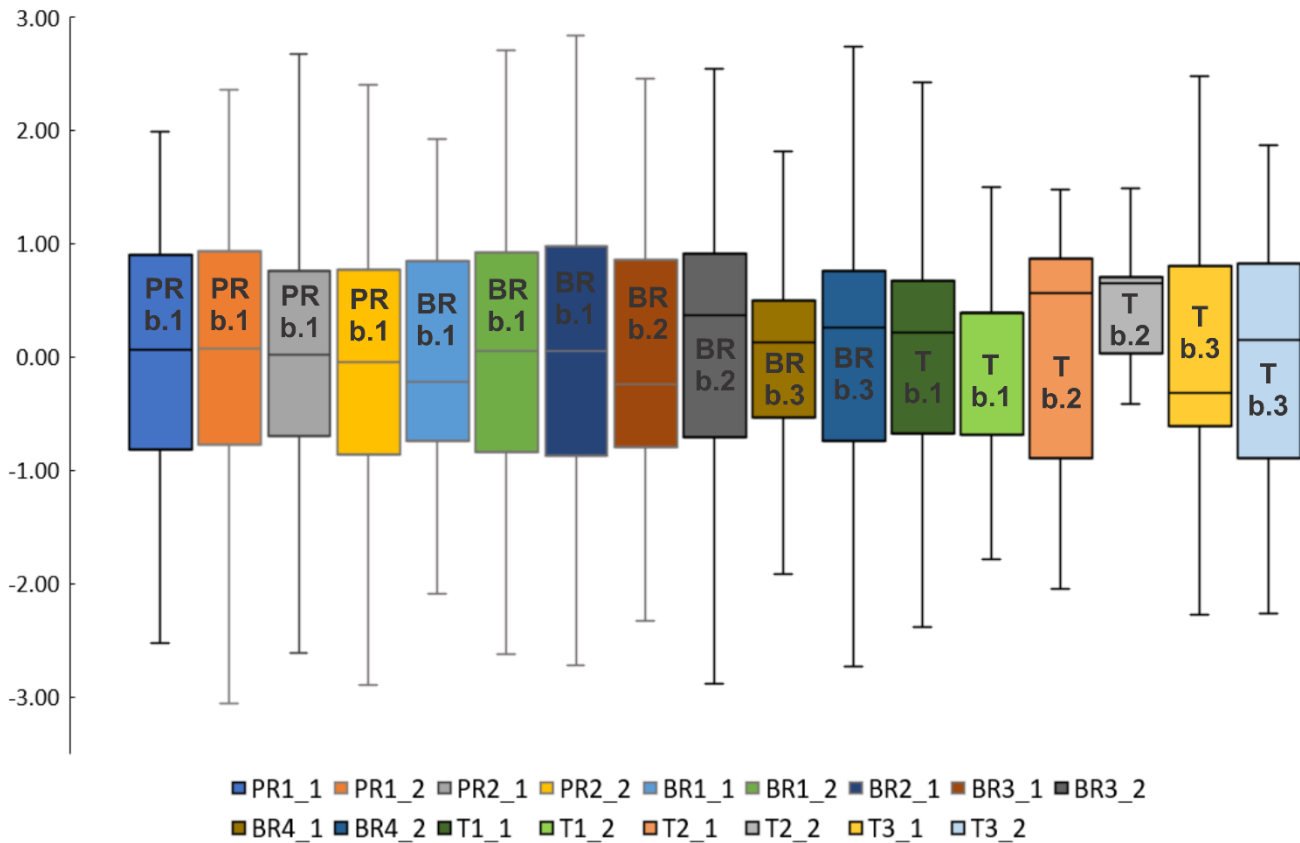
305 The amplitude of crackmeters position differs between individual sites and blocks (Table 4, Fig. 8). These differences are caused by different blocks dimensions, time series length, crackmeters placement and the regime of destabilization.

| Site | Block | Crack meter position amplitude Δl [mm] | | | | measuring since |
|----------------|-------|------------------------------------------------|--------|--------|--------|-----------------|
| | | CM1-P1 | CM1-P2 | CM2-P1 | CM2-P2 | |
| Pastýřská rock | 1 | 1.05 | 0.95 | 0.75 | 0.75 | 23.10.18 |
| Branická rock | 1 | 1.45 | 0.35 | 0.25 | N/A | 4.6.19 |
| | 2 | 0.4 | 0.5 | N/A | N/A | 20.6.19 |
| | 3 | 0.75 | 0.7 | N/A | N/A | 10.7.20 |
| Tašovice | 1 | 0.65 | 0.25 | N/A | N/A | 4.12.18 |
| | 2 | 0.6 | 0.75 | N/A | N/A | 4.12.18 |
| | 3 | 0.85 | 0.7 | N/A | N/A | 18.10.19 |

310 **Table 4: Amplitude of crackmeters measuring at Pastýřská rock: 1 block 4 crackmeters, Branická rock: 3 blocks 7 crackmeters and Tašovice: 3 blocks 6 crack meters. The table shows the difference between maximal and minimal opening of all placed crackmeters. CM: crackmeter, P: position. Amplitude is calculated as difference between maximal and minimal position. By block is meant on which specific block (according to Fig. 3) at each site is instrumented by crack meter. Last measured data: 27.1.2021**

So far, crackmeters amplitudes (Fig. 8, Table 4) higher than 1 mm were measured on Block 1 (approx. 170 m³) at Pastýřská rock site (PR1_1, PR1_2) and on Block 1 (approx. 16 m³) at Branická rock site (BR1_1, BR1_2, BR2_1). These blocks are the two largest instrumented. Measured crackmeter amplitude is reversible and thus caused by block thermal expansion/contraction. The relatively small block 3 at Branická rock site (BR4_1, BR4_2) shows movements larger than 0.5 mm although it is instrumented only since summer 2020. Such a large amplitude suggests that the block is unstable and by further monitoring this hypothesis should be confirmed.

315



320 **Figure 8: Box plots of crackmeters positions data. To compare of different positions of measurements, data were standardised. Boxplots shows max/min of crackmeter position, median, first and third quartile. By abbreviation inside boxplots is defined crackmeter location. PR: Pastýřská rock, BR: Branická rock, T: Tašovice. Block is defined by numbers b.1 – b.3. These corresponds with blocks displayed at fig. 3.**

Blocks that are instrumented at the Tašovice site seems to be more stable (Table 4, Fig. 8). Only Block 3 shows 0.85 mm of reversible movement. By further analyses of graphs and statistical trends analyses possible blocks' irreversible trends

325 should be revealed. Destabilization of the single blocks should be visible as irregularities in the crackmeter position time-series not strictly related to thermal dilatation. Two crackmeters at Tašovice site show large amplitudes of movement (T2_2, T3_2), however, these movements were fully reversible and short lasting (one-hour measurement). They were probably caused by external forces, such as the weight of snow cover deforming the crackmeter body or the deformations of anchoring point during maintenance. Larger blocks (PR b.1, BR b.1; BR b.2) show the largest overall amplitude of movements. The rest of
330 smaller blocks show smaller overall amplitudes. However, these seem to be more influenced by short-term diurnal temperature changes. Sensitivity to fast heating/cooling makes these blocks more susceptible to temperature-induced irreversible movements.

6 Discussion

Commonly used rock stability monitoring systems are often designed to provide an early warning (Jaboyedoff et al.
335 2004, 2011; Crosta et al. 2017), aiming primarily at the identification of a hazard and not to investigate the causes or thresholds of the movement acceleration. The presented monitoring system is designed to contribute to explaining various meteorological and temperature related influences on the destabilizing processes, which lead to the rock fall event triggering (Viles, 2013). Fantini et al. (2017) have concluded that it is the temperature variations (rather than precipitation or wind) that cause changes in internal strain within the rock mass leading to its destabilization. Other factors, such as climate change, former rock fall,
340 seismic stress or hydrological processes are more responsible for rock fall triggering than for short-term strain field modification (Krautblatter and Moser 2009). However, to assess the strain changes within the rock mass, it is necessary to have information on the temperature distribution inside the rock slope depth. This is the crucial advantage of the presented monitoring system, as the borehole compound temperature probe allows identification of short and long-term temperature changes up to 3 m depth.

345 To observe individual thermally-induced strain changes related to rock mass temperature and solar radiation, we have placed the monitoring systems on rock slopes with various slope aspects (different insolation and its diurnal and annual changes) and built of different rocks (sandstone, granite and limestone) to include the influence of heat conductivity, capacity and colour of the rock. While there are numerous laboratory studies on the rock conductivity (Saez Blásquez et al. 2017), modelling of heat flow based on surface observation (Hall and André, 2001, Marmoni et al. 2020), large-scale experiments
350 usually aiming at heat management in the thermal energy industry (Zhang et al. 2018). There are only a few experiments concerning the shallow (first meters) subsurface zone of rock slope (Greif et al. 2017, Magnin et al. 2015a), even though this is the most short term thermally strained and weathered part of the natural rock mass (Marmoni et al. 2020). Moreover, thermal conductivity or rock strength can be determined from heating/cooling rates of rock slope surfaces using a thermal camera (Pappalardo et al. 2016; Pappalardo and D'Olivo, 2019; Fiorucci et al. 2018; Guerin et al. 2019; Loche et al., 2021). Our
355 approach is aiming to combine these methods, with the ultimate goal of creating numerical thermomechanical models of monitored rock slopes/partial unstable blocks.

The analyses of structural properties of the rocks were performed using two approaches: i) traditional field measurements using a geological compass and ii) DSE software for automatic discontinuity extraction from the DSM (Riquelme et al., 2014). While generally the results were similar, the DSM analysis did not include discontinuities that are not forming the surface of the rock face. This effect is visible mainly in the case of the Tašovice rock slope 3D model, where the structural setting is not so straight forward as it is at Branická rock and Pastýřská rock sites, formed by sedimentary rock layers. The proposed monitoring system is compact, built of low-price and easily accessible off-the-shelf components (Tables 1 and 2), and easy to modify according to specific conditions of given site. The performance of the monitoring system is so far without major problems related to the components or general reliability. However, one crackmeter datalogger was damaged and one pyranometer was destroyed by a rockfall triggered by a severe thunderstorm. Maintenance consists of changing datalogger batteries and cleaning rain gauge buckets. Online data transfer via Sigfox IoT network (crackmeters) and GSM (weather stations) works without any issues.

A disadvantage of the used crackmeters is that it only provides one-dimensional displacement data. However, the device is quite low-priced, with good precision and temporal resolution (Table 2) To amend the 1D displacement measurement, we place several crackmeters to each instrumented site. Depending on the spatial configuration of crackmeters, even 3D on the spatiotemporal behaviour of the monitored blocks can be obtained. Additionally, 3D data about larger displacements are acquired using UAV SfM photogrammetry and TLS campaigns.

As concerns the monitoring of the environment, there are clearly observable differences between sites caused by slope aspect and local microclimate. When temperature data from the boreholes are compared, differences between monitored sites are apparent (Fig. 6). Both diurnal (up to approx. 150 cm depth) and annual temperature cycles (up to 3 m depth) for each site can be defined. Differences between these are caused by combination of the different rock slope aspect and by the physical properties of the different rock types. In further research, we plan to use time lapse thermal camera observation to extend the information into whole rock slope surface (Racek et al., 2021).

Solar radiation balance is not directly comparable, due to different aspect and slope of instrumented rock slabs. However, the temporal shift in maximum radiation caused by the rock slope aspect is visible from the solar radiation chart (Fig. 5). When complete annual data about solar radiance will be available (summer/autumn 2021), thorough investigation of the differences will be performed. Consequently, the effects of long-term solar radiation cycles on rock slope dynamics will be possible.

It is necessary to remark that the destabilisation processes are rather slow and have a low magnitude in the central European mid-latitude climate, because of lower temperature amplitudes, shorter period of active freeze-thaw cycles and lower precipitation (Krautblatter and Moore, 2014; Hermans and Longva, 2012; Viles, 2013). Therefore, monitoring is necessary. To observe the processes in more extreme conditions, we have recently installed a new monitoring site in the Krkonoše Mountains (N Czechia) at the altitude of 1270 m a.s.l.. Here we expect to witness the blocks destabilization processes act with greater intensity.

Another factor, contributing to the course of climatic conditions on the observed sites, are various climatic cycles of different length, amplitude and depth-reach, ranging from diurnal cycles up to long-term cycles linked with solar activity or climatic oscillations (Gunzburger et al. 2005; Sass and Oberlechner., 2012; Pratt et al. 2019). Among these the most prominent are diurnal and annual cycles (Marmoni et al. 2020). Diurnal cycles have shallower reach (Fig. 6), but are fast and thus cause intensive strain in the surficial rock layer. Annual cycles are slower, but with higher amplitude and depth reach (Hall and André, 2001). In depth temperature data will help to clarify the role of thermally-induced stress in rock disintegration. Temperature changes causes irregular heating and cooling of rock mass. These leads to irregularities in rock mass dilatation at surface and in depth, which causes thermally induced stress/strain, which eventually can lead to discontinuity evolution and breakage of rock mass surface layers. Thermally-driven disintegration also acts at grain scale where grains of different minerals expand differently and induce stresses in to rock mass (Hall and André, 2001;2003).

On all sites, the highest diurnal measured crackmeter movements are recorded in the spring and autumn months, when diurnal rock slope surface temperature changes have the largest magnitude. The conditions, especially when crossing the freezing temperature twice a day cause the development of freeze-thaw cycles and consequent destabilization of the rock slopes. We expect that the irreversible displacements trends will mostly occur during these periods.

Several works using similar monitoring instrumentation and approaches were published (Matsuoka 2008; Bakun-Mazor et al. 2013,2020; Dreabing, 2020; Draebing et al. 2017; Nishi and Matsuaoka 2010). Despite that, thermally induced rock slope destabilization monitoring is still a relatively marginally studied field. Matsuoka (2008) presented long-term data of crackmeter monitoring. His data were collected on rock slopes in a high mountainous alpine environment. Similarly, to our results the displacement dynamics presented by Matsuoka (2008) influenced by in-situ air and rock mass temperature, reaching the highest values in spring and autumn. On relatively long crackmeter timeseries (10 years) Matsuoka (2008) observed a gradual, temperature-driven joint opening. The most significant Most significant changes in crackmeter position are explained by freeze-thaw conditions. Nevertheless, even in the dynamic alpine environment, a joint opening is slow, measured approx. 0.4 mm in two years of continuous monitoring. It is expected that in temperate climate these processes are even slower. Nishi and Matsuaoka (2010) described the influence of temperature on large rock slide's temporal displacement. They have noted a large displacement (over 1 m) during three years of monitoring, while the accelerations were linked to the highest precipitations periods. However, these values were observed in very different conditions from our experimental sites. Bakun-Mazor et al. (2013, 2020) proposed monitoring system to distinguish thermally and seismically induced joint movements in limestone and dolomites at the Masada cultural heritage site. Measured amplitude of thermally-induced irreversible joint movements reached approx. 0.3 mm in one year. The authors have described concept of thermally-driven wedging-ratcheting mechanism. Estimated annual irreversible joint opening at Masada was approx. 0.2 mm.

We assume, that in the long-term (several years), we will be able to observe a similar wedging-ratcheting mechanism with lower amplitude at our sites. During colder periods, this mechanism can be complemented with frost shattering.

425 Draebing et al. (2017) and Draebing (2020) monitored crack opening in an alpine environment. In this extreme environment, they observed ice wedging driven crack opening up to 1 mm in several days during the snowmelt period. By comparing joint measuring of temperature and dilatation the authors have established the irreversible gradual joint opening of approx. 0.1 mm/year. Our data from the 2020/21 winter period and the newly instrumented site at Krkonoše mountains should show similar results. However, with the lack of active permafrost and permanently ice-filled joints at our sites, these movements should have lower magnitude.

430 Measuring the temperature of dry unfrozen rock mass depth is still a rarely used approach. Magnin et al. (2015a) measured rock mass temperature inside 10 m deep boreholes. This research, however aims at to the estimation of the active permafrost depth and its spatio-temporal behaviour. They have measured annual temperature amplitude approx. 5°C in 3 m depth. Our data from sub-horizontal boreholes show rock mass temperature amplitude of approx. 10°C in the depth of 3 m. This is probably caused by the different climate of our sites.

435 Fantini et al. (2018) studied short-term temperature profiles at experimental limestone quarry rock slope. Diurnal temperature cycles in their case reached a maximum depth of approx. 20-30 cm, which corresponds with our measurements. We can observe diurnal temperature cycles up to 50 cm depth during summer period, when rock mass surface is intensively heated by solar radiation. It is necessary to mention, that comparison of these results is not straight forward due to the diverse climate.

440 Currently, the three sites are continuously measuring for a period between one and two years. Based on this, we can show that the system is capable of observing the influence of thermal stress on the response of the monitored blocks (Fig. 7). However, to exclude seasonality, of the observation period should be longer than 2-3 years. During this period, we expect to observe the process of long-term rock slope destabilization represented by a gradual irreversible trends of crack opening/closing. Longer timeseries will also allow using of statistical trend tests to describe trends in monitored joints dynamics. The influence of meteorological variables on the rock blocks stability will be statistically analysed, to find out how individual meteorological variables influence the dynamic of joints. In-depth temperatures will be analysed to find differences in thermal conductivity, diffusivity and seasonal temperature trends between the monitored sites. Differences in thermo-mechanical behaviour of different rock slopes will be studied using numerical modelling. Furthermore, the monitoring system will be continuously upgraded. Installation of in-situ strain gauges monitoring is planned to directly observe changes in rock mass surface strain.

445
450

7. Conclusions

A newly designed rock slope stability monitoring system was introduced, combining the monitoring of meteorological variables with a 3 m deep in-rock thermal profile and dilatation of the unstable rock block joints. This setup brings a unique opportunity to observe long-term gradual changes within the rock face, leading to the rock slope destabilization.

455 The design of the system allows an easy installation at various locations without major adjustments or changes. All components of the system are available off-the-shelf, at a relatively low price and are easy to replace with low skill requirements. The environmental data are transferred via GSM to a remote server, and the dilatation data are sent via IoT SigFox network or can be downloaded remotely from several tens of meters. Thus, the maintenance visits of the sites can be limited to several months' intervals.

460 The monitored sites are easily comparable as identical monitoring set-up and equipment is used. Thus, we are monitoring the reaction of various rock types on a certain climatic event and observing the differences and similarities on particular sites. This concerns not only movements or expansion of the rock mass but also the heat advance into the rock, its velocity and amplitudes, otherwise very difficult to measure. Significant differences in shallow surface rock mass zone are observable from 3 m borehole thermocouple probe data.

465 Further development of this project should include the installation of in-situ rock surface strain monitoring using in situ placed strain gauges. These data will be used for heat flow and heat-induced strain numerical modelling within the rock mass.

Measuring of joint movements combined with temperature and other external influencing factors will be analysed to understand contribution of individual processes, leading to rock slope destabilization. Whole system will be gradually maintained and placed at other suitable sites to extend the information base and include more possible influencing factors.

470

Data availability

Data available: <https://data.mendeley.com/datasets/4t38tvb4yn/draft?a=f9020d9b-fbd3-4489-a1ca-0e4ffd623212>

Authors contribution

O. Racek, J. Blahůt and F. Hartvich designed system and directed instrumentation of sites and continuously processing data and maintain monitored sites

475

O. Racek processed crack meters data

J. Blahůt processed in-depth temperature data and environmental data

F. Hartvich supervised all works, helped with graphic parts of the manuscript and participated in setting up the monitoring

Competing interests

480 "The authors declare that they have no conflict of interest."

8 Acknowledgements

This research was carried out in the framework of the long-term conceptual development research organisation RVO: 67985891, TAČR project number SS02030023 “Rock environment and resources” within program “Environment for life”,
485 internal financing from Charles University Progress Q44 and SVV (SVV260438) and the Charles University Grant Agency [GAUK 359421]

References

- Ansari, M.K., Ahmed, M., Singh, T.N.R., Ghalayani, I.: Rainfall, A Major Cause for Rockfall Hazard along the Roadways,
490 Highways and Railways on Hilly Terrains in India, in: Engineering Geology For Society And Territory - Volume 1. pp. 457-460. 2015.
- Bakun Mazor, D., Keissar, Y., Feldheim, A., Detournay, C., Hatzor, Y.H.: Thermally-Induced Wedging–Ratcheting Failure Mechanism in Rock Slopes. *Rock Mech Rock Eng* 53, 2521-2538.. <https://doi.org/10.1007/s00603-020-02075-6>, 2020.
- Bakun-Mazor, D., Hatzor, Y.H., Glaser, S.D., Santamarina, J.C.: Thermally vs. seismically induced block displacements in
495 Masada rock slopes. *Int J Rock Mech Min* (1997) 61, 196-211.. <https://doi.org/10.1016/j.ijrmms.2013.03.005>, 2013.
- Barton, M.E., McCosker, A.M.: Inclinomater and tiltmeter monitoring of a high chalk cliff, in: Barton, M. E., And A. M. Mccosker. "Inclinometer And Tiltmeter Monitoring Of A High Chalk Cliff." *Landslides In Research, Theory And Practice: Proceedings Of The 8Th International Symposium On Landslides Held In Cardiff On 26–30 June 2000*. Thomas Telford Publishing, pp. 127-132., 2000.
- 500 Blikra, L., Christiansen, H.H.: A field-based model of permafrost-controlled rockslide deformation in northern Norway. *Geomorphology (Amsterdam)* 208, 34-49.. <https://doi.org/10.1016/j.geomorph.2013.11.014>, 2014.
- Burjanek, J., Gassner-Stamm, G., Poggi, V., Moore, J.R., Faeh, D.: Ambient vibration analysis of an unstable mountain slope. *Geophys J Int* 180, 820-828.. <https://doi.org/10.1111/j.1365-246X.2009.04451.x>, 2010.
- Burjanek, J., Gischig, V., Moore, J.R., Fah, D.: Ambient vibration characterization and monitoring of a rock slope close to
505 collapse. *Geophys J Int* 212, 297-310.. <https://doi.org/10.1093/gji/ggx424>, 2018.
- Coccia, S., Kinscher, J., Vallet, A.: Microseismic and meteorological monitoring of Séchilienne (French Alps) rock slope destabilisatio, in: 3. International Symposium Rock Slope Stability (Rss2016), Nov 2016, Lyon, France.. pp. 31-32., 2016
- Collins, B.D., Stock, G.M., Eppes, M.C.: Progressive Thermally Induced Fracture of an Exfoliation Dome: Twain Harte, California, USA, in: *IRSM Progressive Rock Failure Conference*, 5-9 June, Ascona, Switzerland, 2017.
- 510 Collins, B., Stock, G.M., Rockfall triggering by cyclic thermal stressing of exfoliation fractures. *Nat Geosci* 9, 395-400, <https://doi.org/10.1038/ngeo2686>, 2016.
- Crosta, G.B., Agliardi, F., Rivolta, C., Alberti, S., Dei Cas, L.: Long-term evolution and early warning strategies for complex rockslides by real-time monitoring. *Landslides* 14, 1615-1632, <https://doi.org/10.1007/s10346-017-0817-8>, 2017.

- D'Amato, J., Hantz, D., Guerin, A., Jaboyedoff, M., Baillet, L., Mariscal, A.M.: Influence of meteorological factors on rockfall occurrence in a middle mountain limestone cliff. *Nat Hazard Earth Sys* 16, 719-735. <https://doi.org/10.5194/nhess-16-719-2016>, 2016.
- Dewez, T.J.B., Girardeau-Montaut, D., Allanic, C., Rohmer, J.: Facets: A CloudCompare plugin to extract geological planes from unstructured 3d point clouds, in: *Int Arch Photogramm Vol. 41, Iss. B5. Prague, CZECH REPUBLIC*, pp. 799-804, 2016.
- do Amaral Vargas, E., Velloso, R.Q., Chávez, L.E., Gusmao, L., On the Effect of Thermally Induced Stresses in Failures of Some Rock Slopes in Rio de Janeiro, Brazil. *Rock Mech Rock Eng* 46, 123-134. <https://doi.org/10.1007/s00603-012-0247-9>, 2013.
- Draebing, D.: Identification of rock and fracture kinematics in high Alpine rockwalls under the influence of altitude.. *Earth Surf Dynam Discuss* 1-31. <https://doi.org/https://doi.org/10.5194/esurf-2020-69>, 2020.
- Du, Y., Xie, M.-wen, Jiang, Y.-jing, Li, B., Chicas, S.: Experimental Rock Stability Assessment Using the Frozen–Thawing Test. *Rock Mech Rock Eng* 50, 1049-1053. <https://doi.org/10.1007/s00603-016-1138-2>, 2017.
- Draebing, D., Krautblatter, M., Hoffmann, T.: Thermo-cryogenic controls of fracture kinematics in permafrost rockwalls. *Geophys Res Lett* 44, 3535-3544.. <https://doi.org/10.1002/2016GL072050>, 2017.
- Eppes, M., Magi, B., Hallet, B., Delmelle, E., Mackenzie-Helnwein, P., Warren, K., Swami, S.: Deciphering the role of solar-induced thermal stresses in rock weathering. *Geol Soc Am Bull* 128, 1315-1338. <https://doi.org/10.1130/B31422.1>, 2016.
- Fantini, A., Fiorucci, M., Martino, S., Marino, L., Napoli, G., Prestininzi, A., Salvetti, O., Sarandrea, P., Stedile, L.: Multi-sensor system designed for monitoring rock falls: the experimental test-site of Acuto (Italy). *Rendiconti Online Societa Geologica Italiana* 41, 147-150. <https://doi.org/10.3301/ROL.2016.115>, 2016.
- Fiorucci, M., Marmoni, G.M., Martino, S., Mazzanti, P.: Thermal Response of Jointed Rock Masses Inferred from Infrared Thermographic Surveying (Acuto Test-Site, Italy). *Sensors* 18, 2221. <https://doi.org/10.3390/s18072221>, 2018.
- GEFRAN,: Position Transducers, 1st ed. 25050 PROVAGLIO D'ISEO (BS) ITALY, 2020.
- Girardeau-Montaut, D.: CloudCompare. Retrieved from CloudCompare: <https://www.danielgm.net/cc>, 2016.
- Girard, L., Beutel, J., Gruber, S., Hunziker, J., Lim, R., Weber, S.: A custom acoustic emission monitoring system for harsh environments: application to freezing-induced damage in alpine rock walls. *Geosci Instrum Meth*1, 155-167.. <https://doi.org/10.5194/gi-1-155-2012>, 2012.
- Greif, V., Brcek, M., Vlcko, J., Varilova, Z., Zvelebil, J.: Thermomechanical behavior of Pravcicka Brana Rock Arch (Czech Republic). *Landslides* 14, 1441-1455. <https://doi.org/10.1007/s10346-016-0784-5>, 2017.
- Gruber, S., Hoelzle, M., Haerberli, W.: Permafrost thaw and destabilization of Alpine rock walls in the hot summer of 2003. *Geophys Res Lett*31.. <https://doi.org/10.1029/2004GL020051>, 2004.
- Guerin, A., Jaboyedoff, Michel, Collins, Brian D., Derron, Marc-Henri, Stock, Greg M., Matasci, Battista, Boesiger, Martin, Lefeuvre, Caroline, Podladchikov, Yury Y.: Detection of rock bridges by infrared thermal imaging and modeling. *Sci Rep-UK9*, 13138-13138.. <https://doi.org/10.1038/s41598-019-49336-1>, 2019.

- Gunzburger, Y., Merrien-Soukatchoff, V.: Near-surface temperatures and heat balance of bare outcrops exposed to solar radiation. *Earth Surface Processes and Landforms* 36, 1577-1589. <https://doi.org/10.1002/esp.2167>, 2011.
- 550 Gunzburger, Y., Merrien-Soukatchoff, V., Guglielmi, Y.: Influence of daily surface temperature fluctuations on rock slope stability: case study of the Rochers de Valabres slope (France). *Int J Rock Mech Min* 42, 331-349. <https://doi.org/10.1016/j.ijrmms.2004.11.003>, 2005.
- Hall, K., Andre, M.F.: New insights into rock weathering from high-frequency rock temperature data: an Antarctic study of weathering by thermal stress. *Geomorphology (Amsterdam)* 41, 23-35. [https://doi.org/10.1016/S0169-555X\(01\)00101-5](https://doi.org/10.1016/S0169-555X(01)00101-5), 2001.
- 555 Hall, K., André, M.F.: Rock thermal data at the grain scale: applicability to granular disintegration in cold environments. *Earth Surf Proc Land* 28, 823-836. <https://doi.org/10.1002/esp.494>, 2003.
- Hellmy, M.A.A., Muhammad, R.F., Shuib, M.K., Fatt, N.T., Abdullah, W.H., Abu Bakar, A., Kugler, R.: Rock Slope Stability Analysis based on Terrestrial LiDAR and Scanline Survey on Karst Hills in Kinta Valley Geopark, Perak, Peninsular Malaysia. *Sains Malaysiana* 48, 2595-2604, <https://doi.org/10.17576/jsm-2019-4811-29>, 2019.
- 560 Hermans, R.L., Longva, O.: Rapid rock-slope failures, in: *Landslides: Types, Mechanisms And Modeling*. pp. 59-70, 2012.
- Hoelzle, M., Azisov, E., Barnadum, M., Huss, M., Farinotti, D., Hagg, W., Kenzhebaev, R., Kronenberg, M., Machguth, H., Merkulshin, A., Moldobekov, B., Petrov, M., Saks, T., Salzmann, N., Schone, T., Tarasov, Y., Usubaliev, R., Vorogushyn, S., Yakovlev, A., Zemp, M.: Re-establishing glacier monitoring in Kyrgyzstan and Uzbekistan, Central Asia. *Geosci Inst Meth* 6, 397-418. <https://doi.org/10.5194/gi-6-397-2017>, 2017.
- 565 Chen, T., Deng, J., Sitar, N., Zheng, J., Liu, T., Liu, A., Zheng, L.: Stability investigation and stabilization of a heavily fractured and loosened rock slope during construction of a strategic hydropower station in China. *Eng Geol* 221, 70-81.. <https://doi.org/10.1016/j.enggeo.2017.02.031>, 2017.
- Isaka, B.L.A., Gamage, R.P., Rathnaweera, T.D., Perera, M.S.A., Chandrasekharam, D., Kumari, W.G.P.: An Influence of Thermally-Induced Micro-Cracking under Cooling Treatments: Mechanical Characteristics of Australian Granite. *Energies* 11, 1338, <https://doi.org/10.3390/en11061338>, 2018.
- 570 Jaboyedoff, M., Oppikofer, T., Derron, M.H., Blikra, L.H., Böhme, M., Saintot, A.: Complex landslide behaviour and structural control: a three-dimensional conceptual model of Åknes rockslide, Norway. *Geological Society, London, Special Publications* 351, <https://doi.org/10.1144/SP351.8>, 2011.
- Jaboyedoff, M., Ornstein, P., Rouiller, R.D.: Design of a geodetic database and associated tools for monitoring rock-slope movements: the example of the top of Randa rockfall scar. *Nat Hazard Earth Sys* 4, 187-196.. <https://doi.org/10.5194/nhess-4-187-2004>, 2004.
- Janeras, M., Jara, J.-A., Royan, M.J., Vilaplana, J.-M., Aguasca, A., Fabregas, X., Gili, J.A., Buxo, P., Multi-technique approach to rockfall monitoring in the Montserrat massif (Catalonia, NE Spain). *Eng Geol* 219, 4-20. <https://doi.org/10.1016/j.enggeo.2016.12.010>, 2017.

- 580 Klimes, J., Rowberry, M.D., Blahut, J., Briestensky, M., Hartvich, F., Kost'ak, B., Rybar, J., Stemberk, J., Stepancikova, P.: The monitoring of slow-moving landslides and assessment of stabilisation measures using an optical–mechanical crack gauge. *Landslides* 9, 407-415. <https://doi.org/10.1007/s10346-011-0306-4>, 2012.
- Krautblatter, M., Moser, M.: A nonlinear model coupling rockfall and rainfall intensity based newline on a four year measurement in a high Alpine rock wall (Reintal, German Alps). *Nat hazard earth sys* 9, 1425-1432. <https://doi.org/10.5194/nhess-9-1425-2009>, 2009.
- 585 Krautblatter, M., Moore, J.R.: Rock slope instability and erosion: toward improved process understanding. *Earth Surf Proc Land* 39, 1273-1278. <https://doi.org/10.1002/esp.3578>, 2014.
- Kromer, R., Walton, G., Gray, B., Lato, M.: Development and Optimization of an Automated Fixed-Location Time Lapse Photogrammetric Rock Slope Monitoring System. *Remote Sens-Basel* 11, 1890. <https://doi.org/10.3390/rs11161890>, 2019.
- 590 Lazar, A., Beguž, T., Vulič, M.: Monitoring of the Belca rockfall. *Acta Geotech Slov* 15, 2-15.. <https://doi.org/10.18690/actageotechslov.15.2.2-15.2018>, 2018.
- Li, A., Xu, N., Dai, F., Gu, G., Hu, Z., Liu, Y.: Stability analysis and failure mechanism of the steeply inclined bedded rock masses surrounding a large underground opening. *Tunn Undergr Sp Tech* 77, 45-58.. <https://doi.org/10.1016/j.tust.2018.03.023>, 2018.
- 595 Loche M., Scaringi G., Blahút J., Melis M.T., Funedda A., Da Pelo S., Erbi I., Deiana G., Meloni M.A., Cocco F.: An infrared thermography approach to evaluate the strength of a rock cliff. *Rem Sens* 13 (7), 1265. <https://doi.org/10.3390/rs13071265>, 2021
- Loew, S., Gischig V., Willengerg, H., Alpiger, A., Moore, J.R.: 24 Randa: Kinematics and driving mechanisms of a large complex rockslide. *Landslides: Types, Mechanisms and Modeling* 297-309, DOI:10.1017/CBO9780511740367.025, 2012.
- 600 Loew, S., Gschwind, S., Gischig, V., Keller-Signer, A., Valent, G.: Monitoring and early warning of the 2012 Preonzo catastrophic rockslope failure. *Landslides* 14, 141-154. <https://doi.org/10.1007/s10346-016-0701-y>, 2017.
- Magnin, F., Deline, P., Ravanel, L., Noetzi, J., Pogliotti, P.: Thermal characteristics of permafrost in the steep alpine rock walls of the Aiguille du Midi (Mont Blanc Massif, 3842 m a.s.l). *The Cryosphere* 9, 109-121. <https://doi.org/10.5194/tc-9-109-2015>, 2015.
- 605 Macciotta, R., Martin, C.D., Edwards, T., Cruden, D.M., Keegan, T.: Quantifying weather conditions for rock fall hazard management. *Georisk* 9, 171-186, <https://doi.org/10.1080/17499518.2015.1061673>, 2015.
- Magnin, F., Krautblatter, M., Deline, P., Ravanel, L., Malet, E., Bevington, A.: Determination of warm, sensitive permafrost areas in near-vertical rockwalls and evaluation of distributed models by electrical resistivity tomography. *J Geophys Res-Earth* 120, 745-762.. <https://doi.org/10.1002/2014JF003351>, 2015.
- 610 Ma, C., Li, T., Zhang, H.: Microseismic and precursor analysis of high-stress hazards in tunnels: A case comparison of rockburst and fall of ground. *Eng Geol* 265, 105435.. <https://doi.org/10.1016/j.enggeo.2019.105435>, 2020.

- Marmoni, G.M., Fiorucci, M., Grechi, G., Martino, S.: Modelling of thermo-mechanical effects in a rock quarry wall induced by near-surface temperature fluctuations. *Int J Rock Mech Min* 134.. <https://doi.org/https://doi.org/10.1016/j.ijrmms.2020.104440>, 2020.
- 615 Matano, F., Pignalosa, A., Marino, E., Esposito, G., Caccavale, M., Caputo, T., Sacchi, M., Somma, R., Troise, C., De Natale, G.: Laser Scanning Application for Geostructural analysis of Tuffaceous Coastal Cliffs: the case of Punta Epitaffio, Pozzuoli Bay, Italy. *Eur J Remote Sens* 48, 615-637.. <https://doi.org/10.5721/EuJRS20154834>, 2015.
- Matsuoka, N.: Frost weathering and rockwall erosion in the southeastern Swiss Alps: Long-term (1994–2006) observations. *Geomorphology (Amsterdam)* 99, 353-368.. <https://doi.org/10.1016/j.geomorph.2007.11.013>, 2008.
- 620 Matsuoka, N.: A multi-method monitoring of timing, magnitude and origin of rockfall activity in the Japanese Alps. *Geomorphology (Amsterdam)* 336, 65-76.. <https://doi.org/10.1016/j.geomorph.2019.03.023>, 2019.
- Pappalardo, G., Mineo, S., Zampelli, S.P., Cubito, A., Calcaterra, D.: InfraRed Thermography proposed for the estimation of the Cooling Rate Index in the remote survey of rock masses. *Int J Rock Mech Min (1997)* 83, 182-196.. <https://doi.org/10.1016/j.ijrmms.2016.01.010>, 2016.
- 625 Nishii, R., Matsuoka, N.: Monitoring rapid head scarp movement in an alpine rockslide. *Eng Geol* 115, 49-57.. <https://doi.org/10.1016/j.enggeo.2010.06.014>, 2010.
- Noetzli, J., Pellet, C.: 20 years of mountain permafrost monitoring in the Swiss Alps: key results and major challenges, in: *Egu General Assembly Conference Abstracts*. 2020. p. 10903, 2020.
- Pappalardo, M., D'Olivo, M.: Testing A Methodology to Assess Fluctuations of Coastal Rocks Surface Temperature. *J Mar Sci Eng* 7, 315.. <https://doi.org/10.3390/jmse7090315>, 2019.
- 630 Pasten, C., M. García, M., Cortes, D.D.: Physical and numerical modelling of the thermally induced wedging mechanism. *Geotech Lett* 5, 186-190, 2015.
- Pratt, C., Macciotta, R., Hendry, M.: Quantitative relationship between weather seasonality and rock fall occurrences north of Hope, BC, Canada. *Bulletin of Eng Geol and the Environment* 78, 3239-3251.. <https://doi.org/10.1007/s10064-018-1358-7>,
- 635 2019.
- Racek, O., Blahůt, J., Hartvich, F.: Monitoring of thermoelastic wave within a rock mass coupling information from IR camera and crack meters: a 24-hour experiment on “Branická skála” Rock in Prague, Czechia, in: *Understanding And Reducing Landslide Disaster Risk: Volume 3 Monitoring And Early Warning*. Springer International Publishing, Cham, DOI: 10.1007/978-3-030-60311-3_3, 2021.
- 640 Racek, J.: Use of rock mass classifications for rock fall susceptibility analysis in the conditions of the Bohemian Massif (Bachelor thesis). Praha, 2020.
- Ravanel, L., Magnin, F., Deline, P.: Impacts of the 2003 and 2015 summer heatwaves on permafrost-affected rock-walls in the Mont Blanc massif. *Sci total environ* 609, 132-143.. <https://doi.org/10.1016/j.scitotenv.2017.07.055>, 2017.
- Reiterer, A., Huber, N.B., Bauer, A.: Image-based point detection and matching in a geo-monitoring system. *Allg. Verm.-*
- 645 *Nachr.* 117, 129–139, 2010.

- Riquelme, A., Abelian, A., Tomas, R., Jaboyedoff, M.: A new approach for semi-automatic rock mass joints recognition from 3D point clouds. *Comput geos* 68, 38-52.. <https://doi.org/10.1016/j.cageo.2014.03.014>, 2014.
- Sarro, R., Riquelme, A., Carlos Garcia-Davalillo, J., Maria Mateos, R., Tomas, R., Luis Pastor, J., Cano, M., Herrera, G.: Rockfall Simulation Based on UAV Photogrammetry Data Obtained during an Emergency Declaration: Application at a Cultural Heritage Site. *Remote Sens-Basel* 10, 1923.. <https://doi.org/10.3390/rs10121923>, 2018.
- 650 Sass, O., Oberlechner, M.: Is climate change causing increased rockfall frequency in Austria? *Nat Hazard Earth Sys* 12, 3209-3216.. <https://doi.org/10.5194/nhess-12-3209-2012>, 2012.
- Scaioni, M., Marsella, M., Crosetto, M., Tornatore, V., Wang, J.: Geodetic and Remote-Sensing Sensors for Dam Deformation Monitoring. *Sensors* 18, 3682.. <https://doi.org/10.3390/s18113682>, 2018.
- 655 Saez Blázquez, C., Farfan Martín, A., Martín Nieto, I., Carrasco García, P., Sanchez Perez, L.S., Gonzalez Aguilera, D.: Thermal conductivity map of the Avila region (Spain) based on thermal conductivity measurements of different rock and soil samples. *Geothermics* 65, 60-71, 2017.
- Selby, M.J.: A rock mass strength classification for geomorphic purposes: with tests from Antarctica and New Zealand. *Z Geomorphol* 24, 31-51., 1980.
- 660 Tertium technology: Gego Crack meter. Pisa Italy, 2019.
- Thiele, S. Grose, L., Micklethwaite, S.: Compass: A CloudCompare workflow for digital mapping and structural analysis, in: *Eguga*. p. 5548, 2018.
- Tripolitsiotis, A., Daskalakis, A., Mertikas, S., Hristopoulos, D., Agioutantis, Z., Partsinevelos, P.: Detection of small-scale rockfall incidents using their seismic signature.. *Third International Conference on Remote Sens-Baseland Geoinformation of the Environment* 9535, 1-9, 2015.
- 665 Vasile, M., Vespremeanu-Stroe, A.: Thermal weathering of granite spheroidal boulders in a dry-temperate climate, Northern Dobrogea, Romania. *Earth Surf Proc Land* 42, 259-271.. <https://doi.org/10.1002/esp.3984>, 2017.
- Vaziri, A., Moore, L., Ali, H.: Monitoring systems for warning impending failures in slopes and open pit mines. *Nat Hazards* 55, 501-512.. <https://doi.org/10.1007/s11069-010-9542-5>, 2010.
- 670 Vespremeanu-Stroe, A., Vasile, M.: Rock Surface Freeze-Thaw and Thermal Stress Assessment in two Extreme Mountain Massifs: Bucegi and Măcin Mts. *Revista de Geomorfologie* 12, 2010.
- Vonder Mühl, D., Noetzli, J., Roer, I.: PERMOS—A comprehensive monitoring network of mountain permafrost in the Swiss Alps 1869-1874, 2008.
- Viles, H.: Linking weathering and rock slope instability: non-linear perspectives. *Earth Surf Proc Land* 38, 62-70.. <https://doi.org/10.1002/esp.3294>, 2013.
- 675 Warren, K., Eppes, M.-C., Swami, S., Garbini, J., Putkonen, J.: Automated field detection of rock fracturing, microclimate, and diurnal rock temperature and strain fields. *Geosci Instrum Meth* 2, 275-288.. <https://doi.org/10.5194/gi-2-275-2013>, 2013.
- Weber, S., Beutel, J., Faillettaz, J., Hasler, A., Krautblatter, M., Vieli, A.: Quantifying irreversible movement in steep, fractured bedrock permafrost on Matterhorn (CH). *Cryosphere* 11, 567-583.. <https://doi.org/10.5194/tc-11-567-2017>, 2017.

- 680 Weber, S., Beutel, J., Faillettaz, J., Meyer, M., Vieli, A.: Acoustic and micro-seismic signal of rockfall on Matterhorn., in: 5Th European Conference On Permafrost, Book Of Abstracts. Laboratoire EDYTEM, Université de Savoie Mont-Blanc, pp. 944-945, 2018.
- Weigand, M., Wagner, F.M., Limbrock, J.K., Hilbich, C., Hauck, C., Kemna, A.: A monitoring system for spatiotemporal electrical self-potential measurements in cryospheric environments. *Geosci Instrum Meth*9, 317-336..
685 <https://doi.org/10.5194/gi-9-317-2020>, 2020.
- Westoby, M.J., Brasington, J., Glasser, N.F., Hambrey, M.J., Reynolds, J.M.: ‘Structure-from-Motion’ photogrammetry: A low-cost, effective tool for geoscience applications. *Geomorphology (Amsterdam)* 179, 300-314..
<https://doi.org/10.1016/j.geomorph.2012.08.021>, 2012.
- Yan, Y., Li, T., Liu, J., Wang, W., Su, Q.: Monitoring and early warning method for a rockfall along railways based on
690 vibration signal characteristics. *Sci Rep-UK9*, 6606-6606.. <https://doi.org/10.1038/s41598-019-43146-1>, 2019.
- Yavasoglu, H., Alkan, M.N., Bilgi, S., Alkan, O.: Monitoring aseismic creep trends in the İsmetpaşa and Destek segments throughout the North Anatolian Fault (NAF) with a large-scale GPS network. *Geosci Instrum Meth* 9, 25-40..
<https://doi.org/10.5194/gi-9-25-2020>, 2020.
- Zangerl, C., Eberhardt, E., Perzmaier, S.: Kinematic behaviour and velocity characteristics of a complex deep-seated
695 crystalline rockslide system in relation to its interaction with a dam reservoir. *Eng Geol* 112, 53-67..
<https://doi.org/10.1016/j.enggeo.2010.01.001>, 2010.
- FIEDLER: Elektronika pro ekologii [WWW Document]: URL <https://www.fiedler.company/> (accessed 09.21.2020), 2020.
- Zhang, F., Zhao, J., Hu, D., Skoczylas, F., Shao, J.: Laboratory Investigation on Physical and Mechanical Properties of Granite After Heating and Water-Cooling Treatment. *Rock Mech Rock Eng* 51, 677-694.. [https://doi.org/10.1007/s00603-017-1350-](https://doi.org/10.1007/s00603-017-1350-8)
700 8, 2018.